Deep 2MASS Photometry of M67 and Calibration of the Main Sequence $J-K_S$ Color Difference as an Age Indicator

Ata Sarajedini

Department of Astronomy, University of Florida, Gainesville, FL 32611, USA

ata@astro.ufl.edu

Aaron Dotter

Department of Physics and Astronomy, University of Victoria, Victoria, BC, Canada

dotter@uvic.ca

Allison Kirkpatrick

Department of Astronomy, University of Florida, Gainesville, FL 32611, USA

allison@astro.ufl.edu

ABSTRACT

We present an analysis of Two Micron All Sky Survey (2MASS) calibration photometry of the old open cluster M67 (NGC 2682). The proper motion-cleaned color-magnitude diagram (CMD) resulting from these data extends ~3 magnitudes deeper than one based on data from the point source catalog. The CMD extends from above the helium-burning red clump to a faint limit that is more than 7 magnitudes below the main sequence turnoff in the K_S band. After adopting a reddening of $E(B-V) = 0.041 \pm 0.004$ and a metal abundance of [Fe/H] $= -0.009 \pm 0.009$ based on a survey of published values, we fit the unevolved main sequence of M67 to field main sequence stars with 2MASS photometry and Hipparcos parallaxes. This analysis yields distance moduli of $(m-M)_{K_S} = 9.72$ ± 0.05 and $(m-M)_0 = 9.70 \pm 0.05$, which are consistent with published values. We compare the theoretical isochrones of Girardi et al. and Dotter et al. to the CMD of M67 and comment on the relative merits of each set of models. These comparisons suggest an age between 3.5 and 4.0 Gyr for M67. The depth of the M67 data make them ideal for the calibration of a new age indicator that has recently been devised by Calamida et al.- the difference in $(J-K_S)$ color between the main sequence turnoff (TO) and the point on the lower main sequence where it turns down (TD) and becomes nearly vertical $[\Delta(J-K_S)_{TD}^{TO}]$. Coupled with

deep 2MASS photometry for three other open clusters, NGC 2516, M44, and NGC 6791, we calibrate $\Delta(J-K_S)$ in terms of age and find $\Delta(J-K_S)_{TD}^{TO} = (3.017 \pm 0.347) - (0.259 \pm 0.037)*Log Age (yrs).$

Subject headings: Keywords go here

1. Introduction

Infrared photometry of open clusters holds great promise for many reasons. Most of the effort thus far in this area has been geared toward the study of embedded young star clusters in which the primary goal has been to investigate the star (and planet) forming properties of these systems. The infrared is a natural choice in this regard because of its ability to minimize dust obscuration ($A_K \sim 0.1 A_V$), which is often a problem in these objects as they are still enshrouded in their molecular clouds and preferentially located in the disk of the Milky Way.

An often overlooked use of infrared photometry is in the study of 'normal' open clusters – that is to say – clusters that do not necessarily suffer from extreme levels of foreground extinction. Detailed studies of these clusters in the near-IR are important for a number of reasons. First, they can be used to calibrate the variation of features in the color-magnitude diagram (CMD) with cluster properties such as age, metallicity, and distance. Such a calibration provides a means to determine these properties in clusters of interest using proxies in the CMD. Second, near-IR photometry of low-reddening open clusters is important in order to test the color calibrations of theoretical isochrones. In cases where the models perform poorly, these data provide an empirical set of ridge lines that can be used to interpret the observations and indicate particular areas where the stellar models require improvement. These tests are especially important when the properties of stellar populations in distant galaxies are being investigated by comparing population synthesis models to integrated photometry and spectroscopy.

With regard to providing high quality, well-calibrated photometry for low-reddening open clusters, the Two Micron All Sky Survey (2MASS, Skrutskie et al. 2006), is a significant resource. Because of its all-sky coverage and moderate depth, the 2MASS Point Source Catalog (PSC) contains photometry for countless 'normal' open cluster in the JHK_S passbands. Many studies have taken advantage of the PSC in order to probe a variety of scientific questions (e.g. Grocholski & Sarajedini 2002; An et al. 2007, and references therein). A 2MASS resource that is less frequently utilized is the large collection of pointed calibration data taken to standardize the all-sky photometry. These are described in the work

by Nikolaev et al. (2000) and consist of 35 fields distributed in the northern and southern hemispheres that are observed hundreds of times. One of these fields (No. 90067) contains the well-known, solar age and metallicity open cluster M67 (NGC 2682), which is the subject of the present work.

The paper is organized as follows. In the next section, we describe the 2MASS calibration data that we plan to analyze. The morphological features of the CMD are described in Sec. 3, while the next section is devoted to a description of the main sequence fitting method we employ to derive the distance to M67. Section 5 presents a comparison of the 2MASS near-IR CMD of M67 to two sets of theoretical isochrones that are available in the 2MASS filter set. We combine the deep M67 data with similar photometry for three other open clusters in Sec. 6 and investigate the validity of a new a ge indicator recently unveiled in the literature. Finally, our conclusions are summarized in Sec. 7.

2. Observational Data

The observations of M67 analyzed herein were taken as part of the 2MASS calibration process. They were obtained from the 'Combined 2MASS Calibration Scan' source list available from the 2MASS web site. ¹ The 90067 calibration tile, which includes M67, contains 3771 point sources. Of these, 3413 are flagged as genuine, well-measured stars (i.e. not artifacts and not affected by artifacts); these are measured from averages of the best images available, yielding a photometric limit that is 3 to 4 magnitudes deeper than the 2MASS point source catalog itself.

3. Color Magnitude Diagram

The middle panel of Fig. 1 shows the color-magnitude diagram (CMD) of M67 from the deep 2MASS calibration observations. For comparison, the left panel displays the CMD from the 2MASS PSC over the same area. It is evident from this comparison that the calibration data are not only deeper but also exhibit better-defined cluster principal sequences. In particular, below $K_S\sim15$, we see the main sequence (MS) becoming essentially vertical at $\sim0.6M_{\odot}$ where the J– K_S color starts to become insensitive to effective temperature. Though it presumably exists in all star clusters, this downturn in the MS has only been observed in a few systems because it only appears in cool, dense MS stars whose absolute magnitudes

¹http://www.ipac.caltech.edu/2mass/releases/allsky/doc/seca7_4.html

are below the level reached by most near-IR photometric surveys for objects with distance moduli of ~ 10 or greater. The right panel of Fig. 1 shows the result of combining the 2MASS calibration photometry with the proper motion data of Yadav et al. (2008) and including only stars with a probability of membership greater than 20%. This cleans up the M67 CMD considerably clearly defining its principal sequences. For the remainder of the paper, we will use these proper motion selected data for our analysis.

The downturn in the MS is caused by collisionally induced absorption (CIA) of H_2 molecules that begin to appear in the atmospheres of the high gravity main sequence stars at about 4500 K (Saumon et al. 1994). CIA depletes the flux from the near-IR and pushes it into the optical. Solar metallicity isochrones from Dotter et al. (2008), using synthetic fluxes from PHOENIX model atmospheres, indicate that the downturn begins at $0.6M_{\odot}$ and continues at more or less constant color down below $0.1M_{\odot}$.

There are other prominent features in the M67 CMD. For example, the equal-mass binary sequence which parallels the MS in the range $12 < K_S < 15$ stands-out in the deep M67 CMD. At fainter magnitudes, the photometric sequence of the MS binaries blends in with the single star MS. In addition, the CMD shows a prominent population of blue straggler stars and a small but significant core-helium-burning red clump at $K_S \sim 8.0$ and $(J-K_S) \sim 0.68$.

4. Distance of M67

The deep near-IR CMD of M67 shown in Fig. 1 allows us to derive a new value for the distance to this important cluster. To proceed, however, requires the adoption of a metallicity and a reddening for M67. For these, we turn to the literature where an extensive body of work exists to answer this question. The recent work of Taylor (2007) presents an exhaustive analysis of published reddenings and metallicities for M67. He finds a reddening of $E(B-V) = 0.041 \pm 0.004$ and a metal abundance of $E(B-V) = 0.009 \pm 0.009$. For the purpose of the present paper, we will assume that the abundance of M67 is identically the solar value. In addition, we adopt $E(J-K_S) = 0.53 E(B-V)$ from the work of Cambrésy et al. (2002), which means that $E(J-K_S) = 0.022$.

Armed with these quantities, we can proceed to fit the MS of M67 to the field stars with *Hipparcos* parallaxes and 2MASS photometry. These were assembled by Sarajedini et al. (2004) wherein all of the relevant information is given for each star in their Table 2. The colors of these stars must be corrected for the difference in metallicity between M67 and that of the star. This step is accomplished using the same technique as that described by Sarajedini et al. (2004) and Percival et al. (2003). To be consistent with Percival et al.

(2003), we will use only stars with abundances in the range -0.45 < [Fe/H] < +0.35 for the MS fitting. Furthermore, we exclude HIP 84164, since it is clearly an outlier in the CMDs of Percival et al. (2003). This leaves us with 46 field stars to be used in the MS fitting.

First, the slope of the main sequence in the absolute magnitude range of the field stars is established using the theoretical isochrones of Girardi et al. (2002) on the 2MASS system. This MS slope is then used to offset the color of each field star along a vector with this slope to the value it would have at $M_{K_S} = +4.0$, which is approximately in the middle of the absolute magnitude distribution. These transformed colors are plotted as a function of the known stellar metallicity to produce the diagram shown in Fig. 2. A least squares fit to these data with 2- σ rejection yields (J-K_S) = 0.528 + 0.106[Fe/H] with a root mean square deviation of 0.022 mag in color. The slope of this relation (Δ (J-K_S) / Δ [Fe/H]) is then applied to the colors of the field stars in order to adjust them to an abundance of [Fe/H] = 0.0. We note in passing that the dashed line in Fig. 2 is the result of applying this procedure to Girardi et al. (2002) isochrones converted to the photometric system of Bessell & Brett (1988) suggesting very little difference between the two systems.

We also require a fiducial sequence that best represents the location of the M67 MS in the magnitude range of the field stars (i.e. $3.5 \lesssim M_{K_S} \lesssim 4.5$). For this, we began with the proper motion selected deep M67 photometry shown in the upper panel of Fig. 3 and fit a sequence of points to the MS by eye. These points were then represented by a polynomial and offset in color by the adopted reddening to M67 as shown by the solid line in Fig. 3. The magnitude offset was determined by fitting this MS fiducial to the 46 field stars described above using the magnitude errors as weights. This yields a distance modulus of $(m-M)_{K_S}$ 9.72 ± 0.05 . The resultant fit is shown in the lower panel of Fig. 3. The absolute distance modulus is then $(m-M)_0 = 9.70 \pm 0.05$. The error on these values includes the fitting error (0.010 mag) along with the errors due to uncertainties in the reddening ($\sigma_{E(J-K)} = 0.01$ translates to $\sigma_{(m-M)_K} \sim 0.035$) and the metallicity value of the cluster relative to the field stars ($\sigma_{[Fe/H]} = 0.1$ dex translates to $\sigma_{(m-M)_K} \sim 0.042$). It is important to note that the quoted uncertainty includes only these random errors; systematic errors such as those present in the Lutz-Kelker corrections to the field star parallaxes are not included. In any case, our distance for M67 is approximately in the middle of the range of published values as shown by Sarajedini et al. (2004).

5. Comparison With Theoretical Isochrones

With values for the reddening, distance, and metallicity of M67, it is possible to compare the theoretical isochrones to the CMD in order to examine the robustness of the models at faint magnitude levels, especially where the MS turns down. The two panels of Fig. 4 show the M67 data compared with solar abundance isochrones from Girardi et al. (2002) and Dotter et al. (2008) in the 2MASS photometric system. In both cases, we have adopted the reddening from above but adjusted the distance modulus slightly (within the errors) to fit the main sequence of M67 at $K_S \sim 14$. The Girardi et al. models yield a best fit age of 3.5 Gyr while the Dotter et al. models yield a best fit age of 4 Gyr.

The quality of the isochrone fits is not the same between the Girardi et al. and Dotter et al. models. In particular, the Girardi models seem to incorporate too much core overshooting at the main sequence turnoff, thus leading to a blueward hook that is more pronounced than the data indicates. In addition, in the region of the lower main sequence as temperature decreases, the Girardi models turn downward sooner than the the cluster data. In contrast, the Dotter et al. models reproduce these features more faithfully.

The temperature scales of the two isochrones are in reasonable agreement near the MSTO but around 4500 K they begin to diverge, with the Girardi models becoming considerably hotter than the Dotter models as mass decreases along the MS (see Figure 4 of Dotter et al. 2008). It is this difference in the temperature scales that causes the disagreement seen in the CMDs where the Girardi models begin to turn down at a bluer color. The difference itself is likely due to differences in the adopted physics, primarily the equation of state and low-Temperature opacities (see Dotter et al. 2008, section 5.1 for more details).

6. Calibration of a New Age Indicator

Recently, Calamida et al. (2009) presented a new age indicator that makes use of near-IR J–K colors. The diagnostic exploits the difference in color between the MS turnoff (TO) and the point at which the MS turns down (TD) and becomes nearly vertical $[\Delta(J-K_S)_{TD}^{TO}]$. As age increases, the value of $\Delta(J-K_S)_{TD}^{TO}$ becomes smaller. To be useful, this age diagnostic requires calibration, which is typically done by using theoretical isochrones. However, it is important to test the predictions of the isochrones in this regard by comparing them observational data of open clusters whose ages have been measured independently. In the case of the $\Delta(J-K_S)_{TD}^{TO}$ quantity, deep observations that reach the faint lower main sequence with good precision are required. While this is a challenging prospect in Galactic globular clusters, it is certainly a more tractable goal in open clusters because of their relative proximity.

We begin by exploiting the 2MASS point source catalog looking for nearby open clusters with deep photometry. Two systems appear to have adequate photometry for the identifi-

cation of the turndown on the lower main sequence: NGC 2516 and M44 (NGC 2632). To these, we add the M67 data analyzed here and deep near-IR photometry of the old open cluster NGC 6791 (T. von Hippel et al. 2009, in preparation). The latter were obtained with the Gemini 8-m telescope equipped with the Near-IR Imager (NIRI) instrument. The resultant photometry has been calibrated to the 2MASS system using bright stars in common between the two catalogs.

Figures 5 through 8 illustrate our technique for measuring $\Delta(J-K_S)_{TD}^{TO}$ in these four open clusters. First, we isolate the MS stars that likely belong to the cluster so as to minimize contamination from field stars. This is done by eye with some knowledge of where we expect the main sequence of the cluster to be located. The likely MS stars are shown as the larger points in the lower panels of Figs. 5 through 8. The upper panels of these figures display the color histograms of the likely cluster members in each case. The bluest peak in this distribution is the MS turnoff $[(J-K_S)_{TO}]$ while the reddest one represents the MS turndown $[(J-K_S)_{TD}]$. Gaussian fits to these peaks then yield the adopted values for these quantities, which are given in Table 1. Also listed there are the cluster metallicities and ages from their respective sources. We adopt an uncertainty of 0.1 dex in the logarithm of the ages so that the error in the age of NGC 2516 is ~40 Myr while the error in the age of NGC 6791 is ~1 Gyr.

It is clear from Fig. 5 that determining the MS turnoff color of NGC 2516 is the most problematic because of its sparseness. In this case, we limit ourselves to stars with $K_S < 9$ and derive the histogram shown by the thick dashed line, which is referred to the right-hand ordinate in the upper panel of Fig. 5. This then facilitates the Gaussian fit to determine the TO color for NGC 2516.

Figure 9 shows the variation of $\Delta(J-K_S)_{TD}^{TO}$ with age for the four clusters in our sample. As expected, the quantity $\Delta(J-K_S)_{TD}^{TO}$ decreases as a cluster gets older. A weighted least squares fit to these data (dashed line in the upper panel of Fig. 9) yields $\Delta(J-K_S)_{TD}^{TO} = (3.017 \pm 0.347) - (0.259 \pm 0.037)*Log Age (yrs)$. Thus to achieve a precision of better than 0.1 in the logarithm of the age ($\sim 20\%$ error), the quantity $\Delta(J-K_S)_{TD}^{TO}$ would need to be measured with an error of less than 0.026 mag.

The lines in the lower panel of Fig. 9 represent the predicted behavior based on the Dotter et al. (2008) and Girardi et al. (2002) isochrones for the indicated metallicities. It is clear that, given the uncertainties in the observational quantities, the model predictions are consistent with the data.

While Fig. 9 indicates consistency between model predictions of the relationship between age and $\Delta(J-K_S)$, it is important to consider the limitations and uncertainties in these

predictions. The sensitivity of $\Delta(J-K_S)$ decreases with increasing age. As such, the method is likely to be of more use for measuring the ages of young to intermediate age open clusters. Since these systems are also the ones most likely to have sufficiently deep CMDs, this issue is not a major concern. The $\Delta(J-K_S)$ method may prove useful for extracting ages of young open clusters in highly obscured fields where standard isochrone fitting to the CMD is complicated by significant field star contamination.

Dotter et al. (2008) discuss some of the major differences that can be found among different sets of isochrones for ages and metallicities appropriate for open clusters considered in this paper (see their section 5.1 and Figures 2-5). Particularly important to this discussion are the equation of state—especially for the lower MS and the location of the MS turndown, the treatment of convective core overshoot—for the location of the MSTO at a given age, and the adopted color-effective temperature transformations—for the morphology of the isochrones in the J–K_S CMD. Other factors, such as the adopted solar metallicity and $\Delta Y/\Delta Z$, are relevant as well. Finally, we argue that given its insensitivity to age, the location of the MS turndown in the J–K_S CMD provides an excellent calibration for theoretical models: both the effective temperature scale of the stellar evolution models and the color-effective temperature transformations.

7. Summary and Conclusions

We present an analysis of the 2MASS calibration photometry of the old open cluster M67 (NGC 2682). While the 2MASS PSC has seen broad appeal and utilization, the calibration data has not been widely analyzed. Yet, the M67 CMD resulting from these data is more than 3 magnitudes deeper than the one from the PSC extending to more than 7 magnitudes below the main sequence turnoff of M67. From this diagram, we draw the following conclusions:

- 1) Literature value suggest a mean reddening of $E(B-V) = 0.041 \pm 0.004$ and a metal abundance of $[Fe/H] = -0.009 \pm 0.009$. Using these quantities along with 2MASS photometry and *Hipparcos* astrometry for 46 field stars of known metallicity, we perform main sequence fitting on M67 to determine distance moduli of $(m-M)_{K_S} = 9.72 \pm 0.05$ and $(m-M)_0 = 9.70 \pm 0.05$, which are consistent with published values. Note that the quoted distance uncertainty does not include contributions due to systematic errors such as those associated with the Lutz-Kelker corrections.
- 2) We compare the theoretical isochrones of Girardi et al. (2002) and Dotter et al. (2008) to the 2MASS CMD of M67. Generally speaking, both sets of models reproduce the morphology of the CMD within two magnitudes of the MSTO and brighter. However, the Dotter et al.

models provide a more faithful representation of the of lower MS, including the color of the MS turndown. These comparisons suggest an age of 3.5 (Girardi) or 4.0 (Dotter) Gyr for M67.

3) We combine the 2MASS calibration data for M67, PSC photometry for NGC 2516 and M44, and our own data for the old metal-rich open cluster NGC 6791 in order to calibrate the newly devised age diagnostic of Calamida et al. (2009). The diagnostic - the difference in $(J-K_S)$ color between the main sequence turnoff (TO) and the point on the lower main sequence where it turns down (TD) and becomes nearly vertical $[\Delta(J-K_S)_{TD}^{TO}]$ - becomes smaller for older clusters. We find $\Delta(J-K_S)_{TD}^{TO} = (3.015 \pm 0.347) - (0.259 \pm 0.037)*Log Age (yrs) with a very small dispersion in the fitted points.$

We thank Mike Skrutskie for bringing the deep calibration dataset of M67 to our attention. We are grateful to Ted von Hippel for helpful comments on this manuscript. We also thank an anonymous referee for helpful suggestions that greatly improved the presentation of this paper. A. S. was supported by grant AST - 0606703 from the National Science Foundation. A. K. was partially supported by a Research Experiences for Undergraduates supplemental grant from the National Science Foundation. A. D. acknowledges support from the Canadian Institute for Theoretical Astrophysics and the Natural Sciences and Engineering Research Council of Canada.

REFERENCES

An, D., Terndrup, D. M., Pinsonneault, M. H. 2007, ApJ, 671, 1640

Bessell, M. S. & Brett, J. M. 1988, PASP, 100, 1134

Calamida, A., et al. 2009, in The Ages of Stars, in press

Cambrésy, L., Beichman, C. A., Jarrett, T. H., & Cutri, R. M. 2007, AJ, 123, 2559

Claver, C. F., Liebert, J., Bergeron, P., & Koester, D. 2001, ApJ, 563, 987

Dotter, A., Chaboyer, B. Jevremović, D., Kostov, V., Baron, E., & Ferguson, J. W. 2008, ApJS, 178, 89

Girardi, L., Bertelli, G., Bressan, A., Chiosi, C., Groenewegen, M. A. T., Marigo, P., Salasnich, B., & Weiss, A., 2002, A&A, 391, 195

Grocholski, A. & Sarajedini, A. 2002, AJ, 123, 1603

Nikolaev, S., Weinberg, M. D., Skrutskie, M. F., Cutri, R. M., Wheelock, S. L., Gizis, J. E., & Howard, E. M. 2000, 120, 3340

Percival, S. M., Salaris, M., & Kilkenny, D. 2003, A&A, 400, 541

Sarajedini, A. 1999, AJ, 118, 2321

Sarajedini, A., Brandt, K., Grocholski, A. J., & Tiede, G. P. 2004, AJ, 127, 991

Saumon, D. 1994, in "The equation of state in astrophysics," Proceedings of IAU Colloquium No. 147 (Cambridge: Cambridge University Press), edited by G. Chabrier and E. Schatzman, Evry, p.306

Skrutskie, M. et al. 2006, AJ, 131, 1163

Taylor, B. J. 2007, AJ, 133, 370

Terndrup, D. M., Pinsonneault, M., Jeffries, R. D., Ford, A., Stauffer, J. R., & Sills, A. 2002, ApJ, 576, 950

Yadav, R. K. S., Bedin, L. R., Piotto, G., Anderson, J., Cassisi, S., Villanova, S., Platais, I., Pasquini, L., Momany, Y., & Sagar, R. 2008, A&A, 484, 609

This preprint was prepared with the AAS LATEX macros v5.2.

Table 1. Open Clusters

Name	[Fe/H]	Log Age (yrs)	Age Reference	$(J-K_S)_{TO}$	$(J-K_S)_{TD}$	$\Delta (\mathrm{J-K}_S)_{TD}^{TO}$
NGC 2516	$+0.06 \pm 0.03^{a}$	8.15	Terndrup et al. (2002)	-0.002 ± 0.037 0.114 ± 0.041 0.328 ± 0.028 0.451 ± 0.023	0.900 ± 0.061	0.902 ± 0.071
NGC 2632 (M44)	$+0.057 \pm 0.022^{b}$	8.78	Claver et al. (2001)		0.866 ± 0.027	0.752 ± 0.049
NGC 2682 (M67)	-0.009 ± 0.009^{c}	9.60	Sarajedini (1999)		0.856 ± 0.020	0.528 ± 0.034
NGC 6791	$+0.39 \pm 0.05^{d}$	9.98	Sarajedini (1999)		0.888 ± 0.029	0.437 ± 0.037

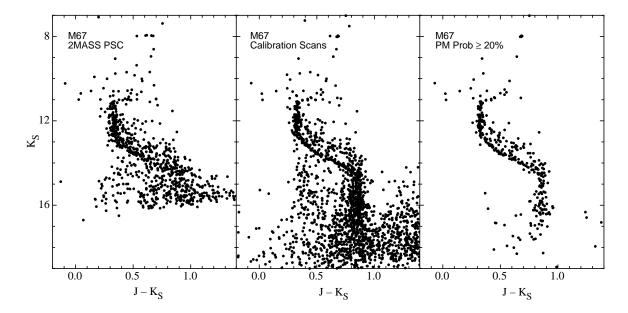


Fig. 1.— The color-magnitude diagram of M67 from the 2MASS point source catalog (left panel) and the Combined Calibration database (middle panel). The right panel also shows the Combined Calibration data but including only stars with a $\geq 20\%$ probability of membership based on the proper motions of Yadav et al. (2008).

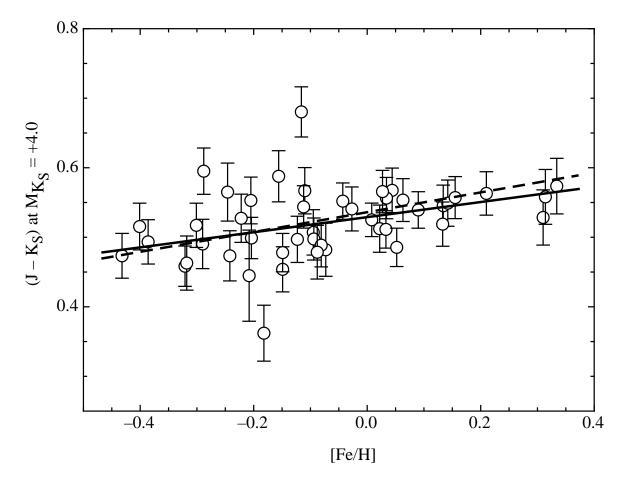


Fig. 2.— The color each field star would have at $M_{K_S} = +4.0$ as a function of the metal abundance for 46 stars with $-0.45 < [{\rm Fe/H}] < +0.35$ from the work of Sarajedini et al. (2004). The solid line is the least squares fit with 2- σ rejection applied. The slope of the fitted line is $\Delta(J-K)$ / $\Delta[Fe/H] = 0.106$. For comparison, the dashed line represents the result of performing this experiment after transforming the 2MASS photometry to the system of Bessel & Brett (1988) suggesting very little difference between the two systems.

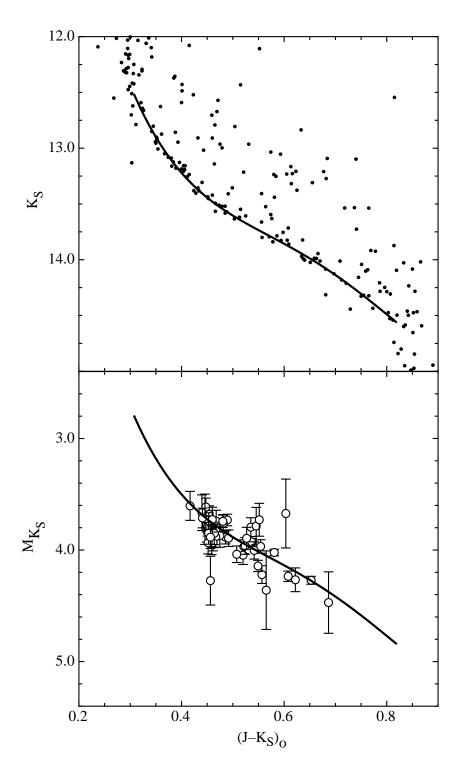


Fig. 3.— The upper panel shows the proper motion selected deep M67 2MASS photometry (filled circles) corrected for a reddening of E(B-V)=0.041. The solid line is the adopted fiducial for the main sequence. The open circles in the lower panel are the field stars with *Hipparcos* parallaxes and 2MASS photometry corrected for distance. The solid line is the M67 fiducial from the upper panel fitted to the field stars resulting in an inferred distance of $(m-M)_{K_S}=9.72$.

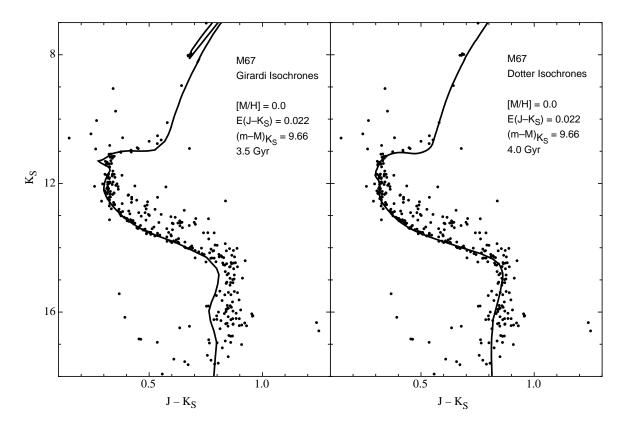


Fig. 4.— The color-magnitude diagram of M67 from the proper motion selected 2MASS Combined Calibration database compared with theoretical models for given values of reddening, distance, and metallicity. The left panel shows the 3.5 Gyr isochrone from Girardi et al. (2002). The right panel displays the 4.0 Gyr track from Dotter et al. (2008).

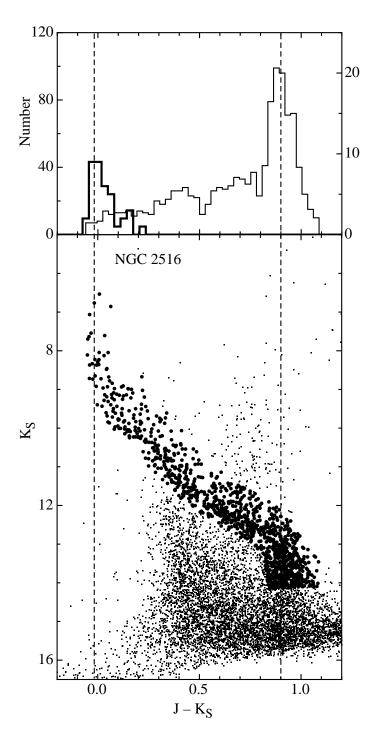


Fig. 5.— The lower panel shows the color-magnitude diagram of NGC 2516 from the 2MASS Point Source Catalog. The larger points denote the stars used to construct the color function shown in the upper panel. Because of the sparseness of the main sequence turnoff region, we further limit the color function in this region to stars with $K_S < 9$. Note that this latter histogram is referred to the right hand ordinate axis. The dashed lines represent the locations of the main sequence turnoff color and the turndown color (see text).

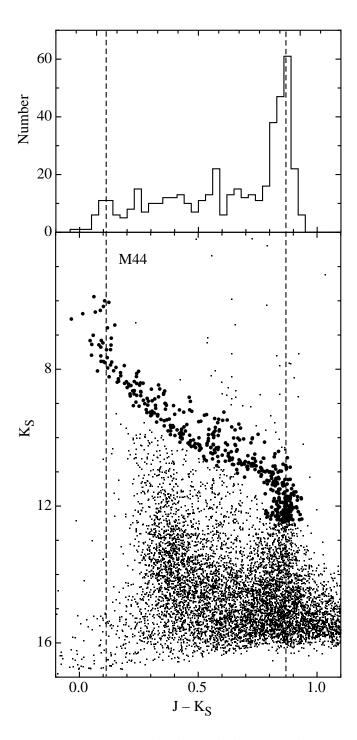


Fig. 6.— Same as Fig. 5 except that the plotted data are the M44 photometry from the 2MASS Point Source Catalog.

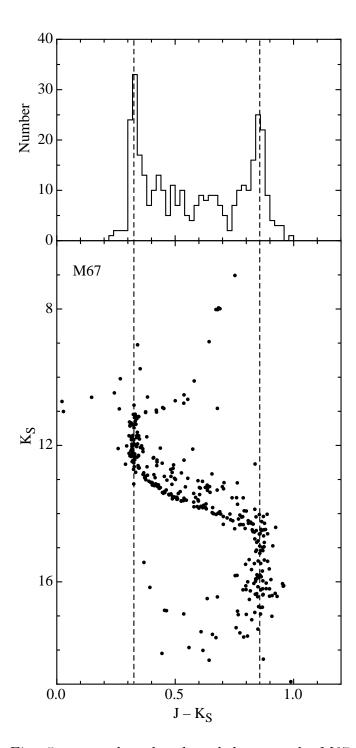


Fig. 7.— Same as Fig. 5 except that the plotted data are the M67 photometry from the proper motion selected 2MASS Combined Calibration database.

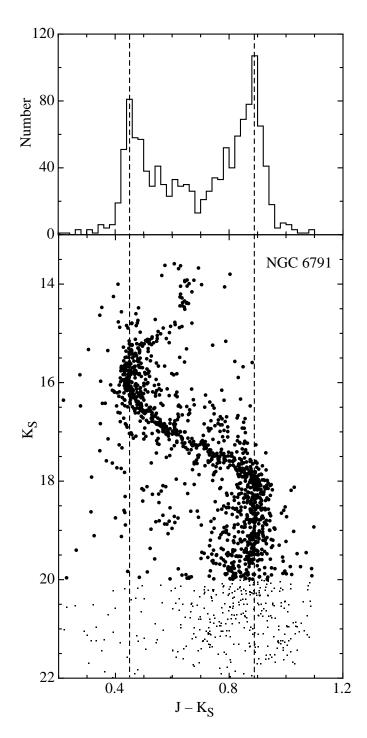


Fig. 8.— Same as Fig. 5 except that the plotted are the NGC 6791 photometry from von Hippel et al. (2009, in preparation).

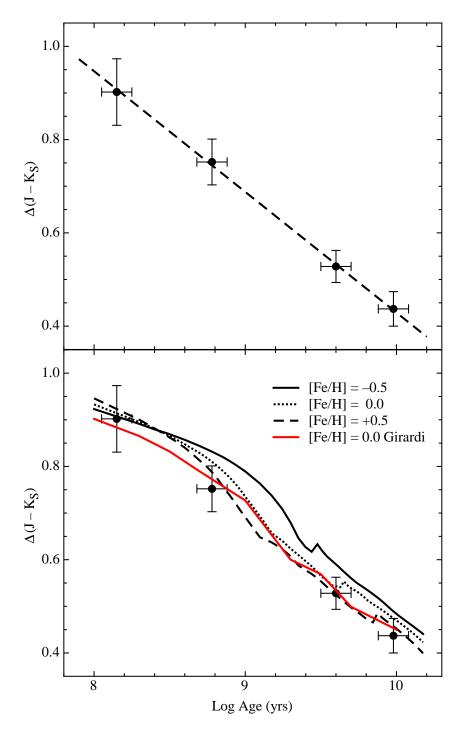


Fig. 9.— The upper panel shows the variation of $\Delta(J-K_S)_{TD}^{TO}$ with the logarithm of the age in years for the clusters in Table 1. The dashed line is the weighted least squares fit to the data. The lower panel displays the same data points but this time compared with the theoretical models of Dotter et al. (2008, black lines) and Girardi et al. (2002, red line).